TRANSPORTATION POOLED FUND PROGRAM
QUARTERLY PROGRESS REPORT

Lead Agency (FHWA or State DOT): ____Kansas DOT_____

INSTRUCTIONS:

Project Managers and/or research project investigators should complete a quarterly progress report for each calendar quarter during which the projects are active. Please provide a project schedule status of the research activities tied to each task that is defined in the proposal; a percentage completion of each task; a concise discussion (2 or 3 sentences) of the current status, including accomplishments and problems encountered, if any. List all tasks, even if no work was done during this period.

Transportation Pooled Fund Program Project # **TPF-5(328)**	Transportation Pooled Fund Program - Report Period: ☐Quarter 1 (January 1 – March 31) ☐Quarter 2 (April 1 – June 30) ☒Quarter 3 (July 1 – September 30) ☐Quarter 4 (October 1 – December 31)
Project Title: Strain-based Fatigue Crack Monitoring of Steel Bridges using Wireless Elastomeric Skin Sensors	
Project Manager: **Susan Barker, P.E.** Phone: (785) 291-3847 E-mail: SusanB@ksdot.org	
Project Investigator: Li Jian Phone: 785-864-6850 E-mail: jianli@ku.edu	

Lead Agency Project ID: RE-0699-01	Other Project ID (i.e., contract #):	Project Start Date: 9/2015
Original Project End Date: Multi-year project	Current Project End Date: 8/31/2018	Number of Extensions: N.A.

Project schedule status:

☒ On schedule   ☐ On revised schedule   ☐ Ahead of schedule   ☐ Behind schedule

Overall Project Statistics:

Total Project Budget	Total Cost to Date for Project	Total Percentage of Work Completed
$405,000	**$ 98,890.09**	**33%**

Quarterly Project Statistics:

Total Project Expenses This Quarter	Total Amount of Funds Expended This Quarter	Percentage of Work Completed This Quarter
$ 32,101.57	**$ 32,101.57**	**8%**

Project Description:
The main objective of this proposed research is to *provide state DOTs a practical and cost-effective long-term fatigue crack monitoring methodology using **a wireless elastomeric skin sensor network**.* This research is intended to demonstrate the value-added of fatigue crack monitoring of steel bridges using wireless skin sensors over the traditional bridge inspection.

Progress this Quarter (includes meetings, work plan status, contract status, significant progress, etc.):

ISU Progress:

Under this task, fatigue crack sensors are to be produced with an approximate thickness of 100-200 μm to enhance the mechanical robustness under harsh environment. Acceptable range of capacitance is 800-1000 pF. The anticipated number of sensors is 150 to 200 for the duration of the project. Fabricated sensors are listed in Table 1.

KU Progress:

The KU team carried out four tasks during this quarter, including 1) a replicated test of the SEC sensor to investigate the reduced signal amplitude when a lower load is applied for measurement than for generating the crack, as reported in the last quarterly report; 2) an investigation of signal processing strategy for more realistic traffic loading; 3) a numerical methodology to predict the SEC's response with different sizes of sensing area, and 4) experimental test to understand the threshold of stress range for crack detection using the SEC sensor.

UA Progress:

During this quarter, the UA team evaluated the performance of the capacitive strain sensor board when it is used with smaller-size (i.e. 1 in x 1 in) SEC sensors. Although the coverage area of the SEC sensor becomes smaller, the lower nominal capacitance of the mini SEC sensor makes the Wheatstone bridge of the sensor board better balanced, allowing higher gain of signal. Higher gain signals are expected to have less noise and more sensitive to low-level strain signal from structures.

Arizona team has improved the capacitive strain sensor board to be used for grounded configuration of SEC sensor to achieve less noise, and conducted series of shear building tests on the shake table to evaluate the performance.

Table 1 – produced sensors

Sensor	Date cast:	Capacitance (pF)	Dielectric Thickness (mm)	std dev	Resistance (kOhm)
61-63		Info not available			
64	5/8/2016	823	0.162	0.0058	17.8
65	5/8/2016	792	0.168	0.0075	18.3
66	5/8/2016	796	0.163	0.0067	18.0
67	5/8/2016	826	0.157	0.0085	17.5
68	5/8/2016	800	0.165	0.0085	18.2
69	5/8/2016	863	0.144	0.0094	17.4
70	5/8/2016	854	0.168	0.0071	17.2
71	5/8/2016	813	0.152	0.0034	18.2
72	5/8/2016	886	0.153	0.0053	16.9
73	5/8/2016	867	0.150	0.0071	17.4
74	5/8/2016	848	0.156	0.0101	17.7
75	6/14/2016	829	0.158	0.0048	18.2
76	6/14/2016	847	0.151	0.0091	18.2
77	6/14/2016	801	0.162	0.0053	19.7
78	6/14/2016	839	0.151	0.0080	18.8
79	6/14/2016	830	0.147	0.0067	18.9
80	6/14/2016	855	0.156	0.0076	18.3
81	6/14/2016	828	0.159	0.0076	19.3
82	6/15/2016	800	0.160	0.0071	18.9
83	6/15/2016	827	0.151	0.0080	18.5
84	6/15/2016	820	0.155	0.0053	18.6
85	6/15/2016	823	0.147	0.0033	18.2
86	6/15/2016	848	0.150	0.0047	17.4
87	6/16/2016	839	0.159	0.0039	18.6
88	6/16/2016	804	0.154	0.0050	19.8
89	6/16/2016	814	0.161	0.0046	18.8
90	6/16/2016	841	0.153	0.0067	18.3

Anticipated work next quarter:

ISU: The objective of the next quarter is to produce 45 additional sensors, for a total of 105 sensors. The production of sensors will continue until KU provides results from testing, which could lead to additional optimization (Task 2). Technical support (Task 3) is being provided to KU on a continuous basis, as well as discussion and feedback (Task 4).

KU: KU team will continue to finish the threshold test in the next quarter, and experimentally verify the proposed data processing strategy under more realistic traffic loading.

UA: In the next quarter, the University of Arizona team will focus on the prototype design of the improved capacitive strain sensor board for the grounded SEC configuration and the interface board to be used with the wireless sensor platform.

Significant Results:

Part one: Fatigue crack detection with the SEC sensor

The KU team performed four tasks in this quarter, including a replicated experimental test of the SEC sensor; an investigation on more realistic traffic loads; a numerical simulation for predicting the sensor's response under different sensing sizes, and a threshold test of the sensor.

The first task is the replicated test. The purpose of this test is to confirm the phenomenon observed in the previous test. Last quarter, the sensor was tested on a compact specimen with different stress ratios. The sensor's ability of crack monitoring is represented in terms of the damage index vs. crack length. In the result, we found an outlier when R = 0.1. The test was repeated to confirm the occurrence of the outlier when R is 0.1 during measurement, which is lower than R = 0.6 for propagating the crack.

The replicated test was performed using the same loading protocol as the one in the last quarter. Fig. 1 shows the loading protocol, where the crack was generated under a higher stress ratio (R = 0.6). During the test, the actuator was paused under each 1/16 in. of crack growth, and data were collected using three different levels of stress ratio (R = 0.1, 0.4, and 0.6).

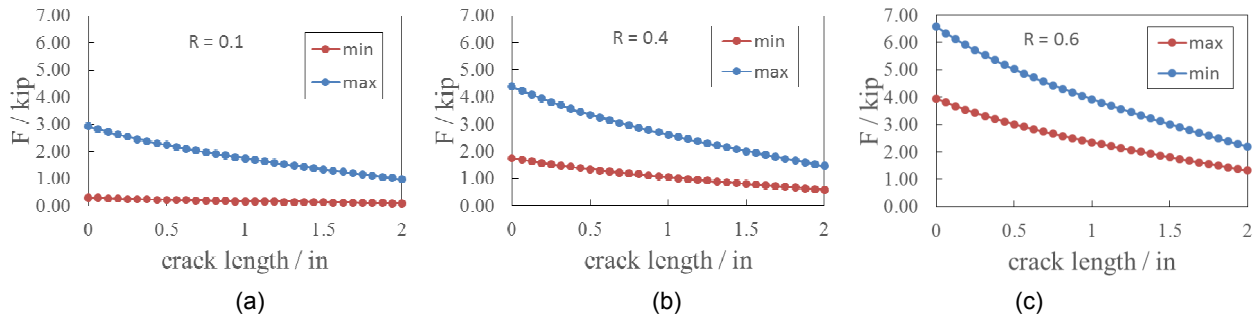(a)   (b)   (c)

Fig. 1 Loading protocols in the replicated test

Fig. 2 summarizes the results of the replicated test and compares the new data with old test results. The blue line is the test result in March, where both the crack propagation and data collection were conducted using R = 0.1; the black lines are the results in August (last quarter), where an outlier is found when R = 0.1; the red lines are the replicated test results.

As shown in Fig. 2, most test results fit in a single straight line, indicating the sensor is able to monitor the crack propagation by showing consistent increase of the damage index. However, two outliers can be found in the figure, one from the original test in August and the other from the replicated test in this quarter. It confirms that the sensor produces lower damage index under a lower stress ration (R = 0.1) in these two tests. A possible explanation is the SEC experienced plastic deformation within the crack region under R = 0.6. When the load ratio is lowered, the sensor within the crack region is not able to return to its original size, leading to lower signal output at the loading frequency.
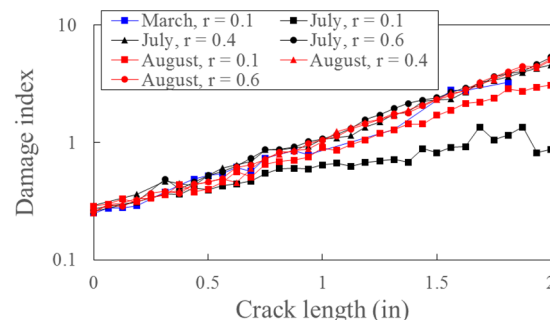

Fig. 2 Summary of results in different tests

The second task of the KU team is investigation of SEC sensor under realistic traffic load. So far, periodic sine waves have been used in the loading protocols. To implement the SEC sensor to steel bridges, the sensor's crack detection ability needs to be verified under a more complex traffic load. Typically, a realistic traffic load would include a series of cycles caused by vehicles with different weights and speeds, leading to different peak-to-peak amplitude and duration of each cycle.

A revised damage index is proposed for more realistic traffic loads, as shown below:

$$damage\ index = \sqrt{PSD_{SEC}}/\sqrt{PSD_{Load}}$$ (Equation 1)

In which PSD_{SEC} is the power spectrum density (PSD) of the sensor's measurement, and PSD_{Load} is the PSD of the excitation load, which, in practical applications, can be represented by a sensor reading from uncracked region. The revised damage index is now looking at a particular frequency range, instead of one single frequency in the previous approach.

A preliminary experimental verification is conducted. A new loading protocol is created as shown in Table 1, which consists of four loading cycles. Each cycle has a different peak-to-peak amplitude and duration/freqency, simulating a different weight and speed of vehicle. Fig. 3 shows the time history of the excitation load.

Table 1 A new loading protocol for traffic load investigation

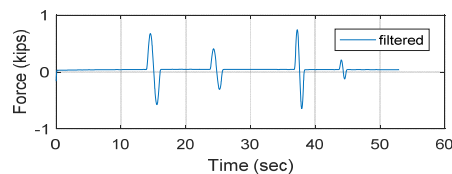| Cycle	Peak-to-peak amplitude (Kips)	Natural frequencies (Hz)
1st	0.52	0.5
2nd	0.3	0.55
3rd	0.59	0.72
4th	0.15	0.98

Fig. 3 Loading history

The aforementioned loading protocol has been applied to the compact specimen when the crack length reached 28/16 in and 32/16 in, respectively. Both SEC sensor's measurement and load measurement were collected. Then, PSD of these measurements are obtained, as shown in Fig.4. An averaging filter is applied to smooth these PSD curves (Fig. 5). Finally, based on Equation 1, the damage index can be computed for the frequency range where the PSD peak locates. The result in Fig. 6 clearly shows that the damage index under 32/16 in crack length is larger than 28/16 in crack length, verifying the sensor's ability to monitor crack growth under a more realistic traffic load.
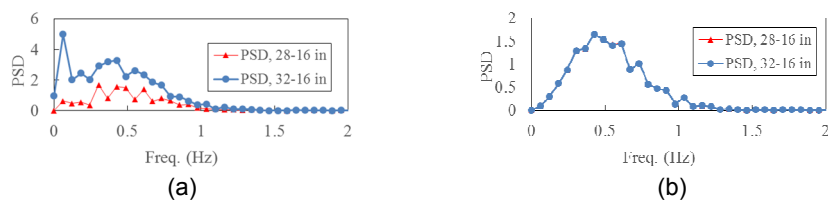

Fig. 4 (a) PSD curves of the SEC sensor; and (b) PSD curve of the excitation load
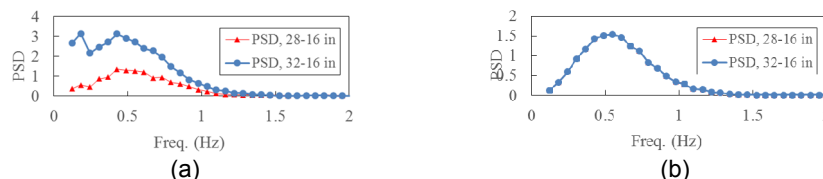

Fig. 5 (a) PSD curves of the SEC sensor after smoothing; and (b) PSD curve of the excitation load after smoothing
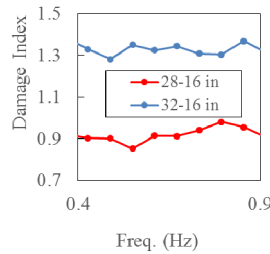
Fig. 6 Damage index

The third task is to apply a numerical approach to study the SEC sensor with difference sensing areas. The purpose is to understand the optimal size of the SEC sensor for crack monitoring using a finite element (FE) modeling approach.

The simulation method includes two steps: 1) an FE model of a compact specimen is created to simulate the crack growth; and 2) the SEC sensor's electronic response is derived using a proposed algorithm. Fig. 7 shows the simulated crack propagation in the FE model. Based on the FE result, an algorithm is applied to compute the capacitance change within the sensing area. Fig.8 shows the comparison between the simulation and test results, which validated the numerical approach to accurately predict the sensor's response under cracking.

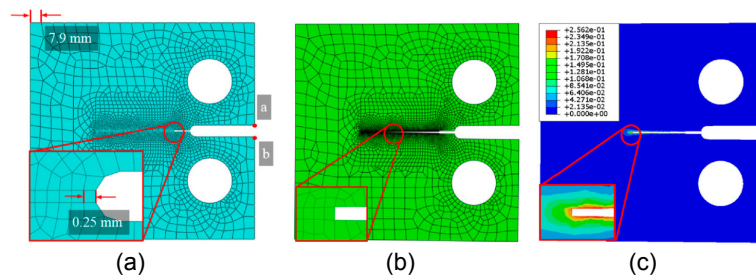(a)　　　　　　　　　(b)　　　　　　　　　(c)

Fig. 7 (a) FE model; (b) crack growth simulation; and (c) plastic strain at the tip of the crack
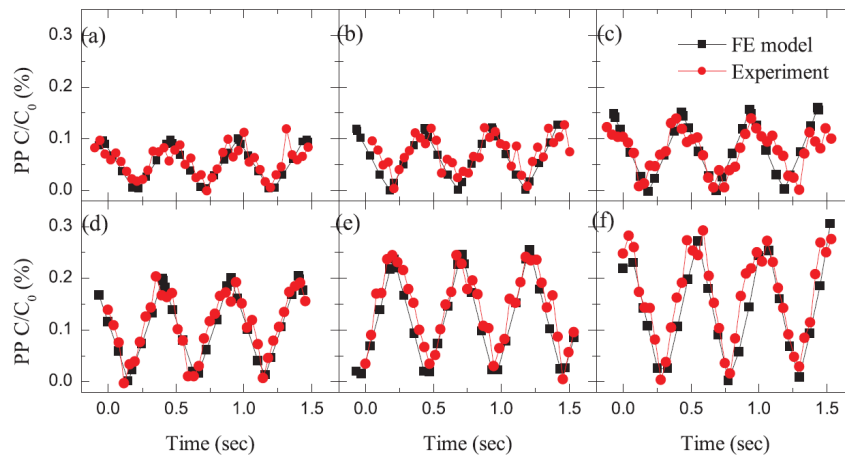

Fig. 8 Simulated capacitance vs. experimental results: where the crack length (measured from the boundary of the sensor) are (a) 1.6 mm; (b) 4.8 mm; (c) 7.9 mm; (d) 11.1 mm; (e) 14.3 mm; and (f) 17.5 mm

Further FE analysis was carried out for different sensor sizes. As shown in Fig. 9, four different sizes of the sensor are investigated. Fig. 9a shows the standard size of the SEC sensor, which is the size used in current experimental tests, as well as two smaller sizes.
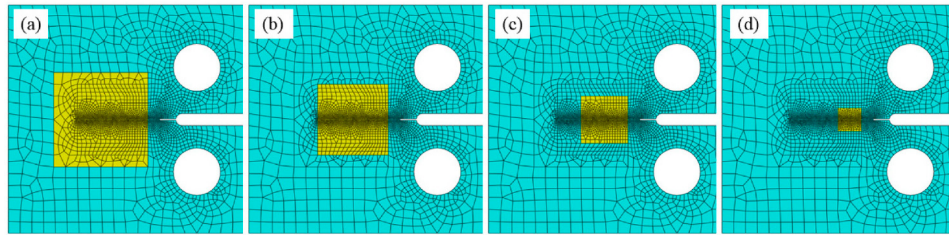
Fig. 9 FE models with different sizes of sensing area, including (a) 2.5 × 2.5 in.^{2} (full size); (b) 1.875 × 1.875 in.^{2} (56% size); (c) 1.25 × 1.25 in.^{2} (25% size); and (d) 0.625 × 0.625 in.^{2} (6% size).

Using the same numerical method, the results of different sizes of the sensors are shown in Fig. 10 in terms of two variables: percentage change of the capacitance (PP C/C_0) and relative change of the capacitance (PP C). The conclusion is that smaller sensor produces less relative capacitance change; however, it is more sensitive to the crack by showing a much higher percentage change of capacitance. The size of sensor, therefore, needs to be optimized to cover strategic areas to achieve desired resolution.
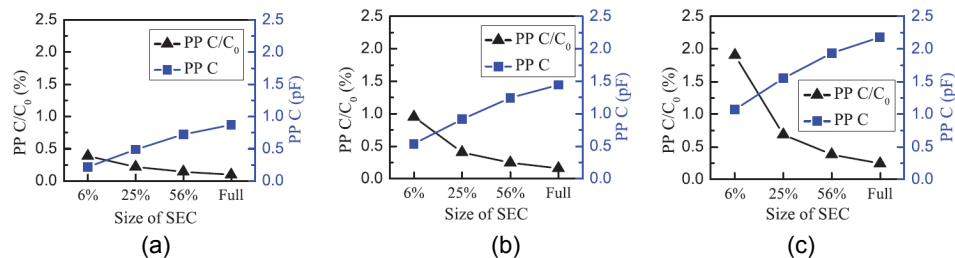

Fig. 10 Capacitance change in terms of PP C/C0 and PP C for different sizes of sensor when the crack reaches different lengths: (a) 1/16 in., (b) 5/16 in., and (c) 9/16 in.

The last task of the KU team is the threshold test of the sensor's ability for crack monitoring. The loading protocol of the threshold test is shown in Fig. 11. The load is featured by four stages with decreasing stress intensity from 10 to 2.5. Instead of continually decreasing the mean load as the previous test, we decided to keep the mean load as constant in this test, representing the dead load in real applications. The test is ongoing and no crack has initiated yet.
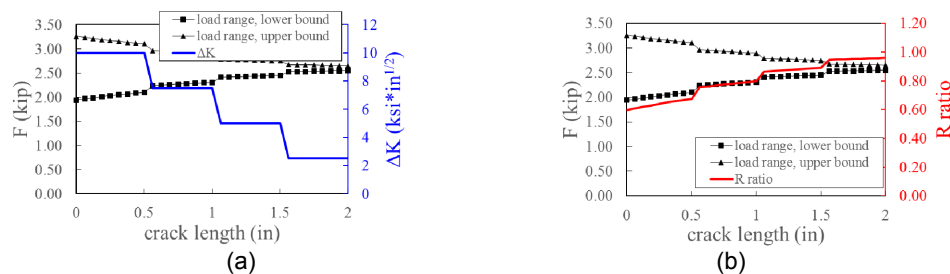

Fig. 11 Loading protocol of the threshold test: (a) ranges of the stress intensity factor and load; and (b) the corresponding stress ratio

Part two: Data acquisition sensor board development for the SEC sensor

1. Performance evaluation of the capacitive strain sensor board with smaller SEC sensors
   As shown in Fig 12, two 1 inch by 1 inch SEC sensors have been installed on a column of a shear building model. The SEC sensors are connected to the strain sensor board and the processed signal (from strain to analog voltage signal) from the sensor board is fed to the 24bit NI DAQ. To minimize noises, minimal-length wires are used and the wires are firmly attached to the shear building member.
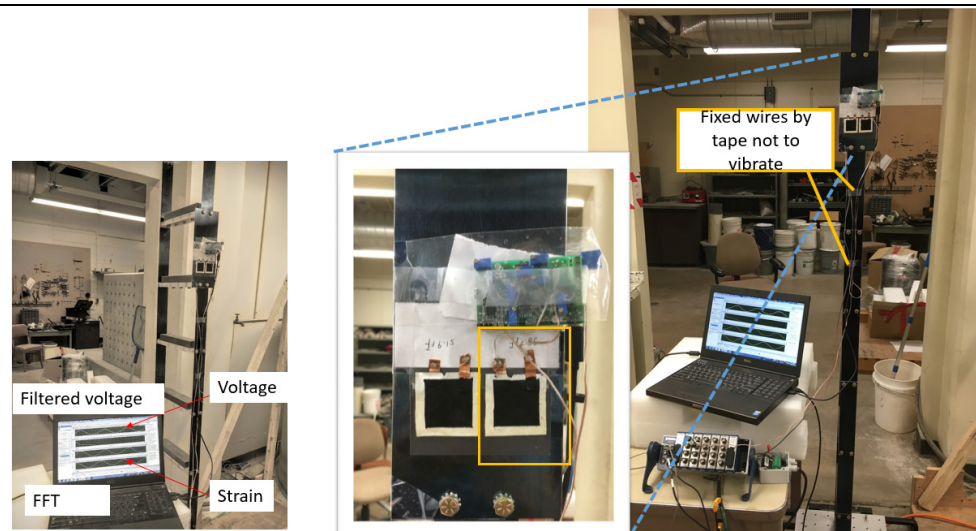
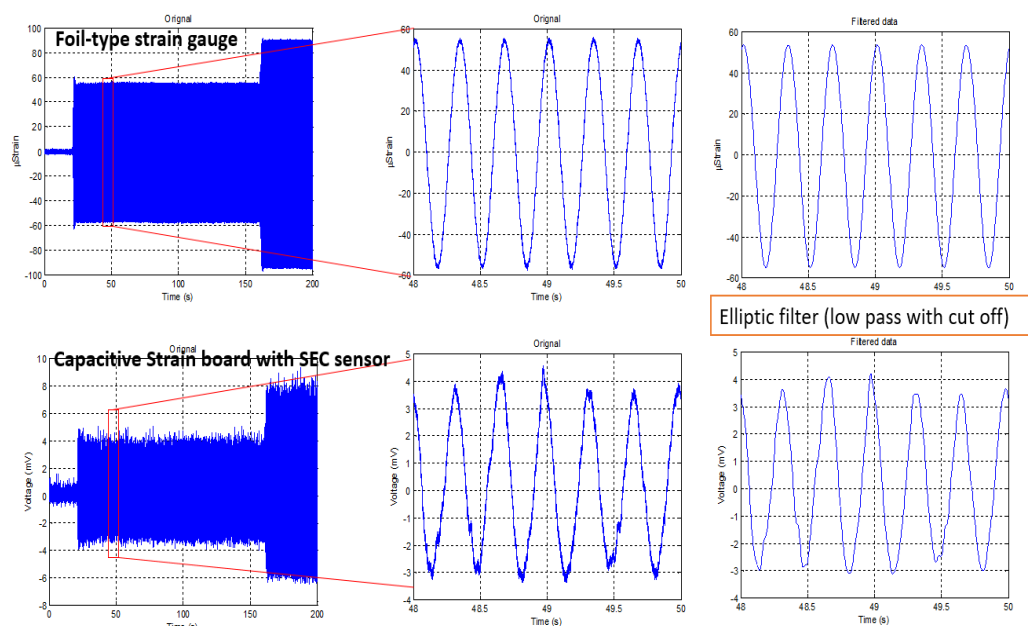Fig 12. Shear building test setup on an electrodynamic shaker

Fig 13. Example measurements from the shear building tests

Fig. 13 shows example measurements from the shear building tests on the shaker. The top row is from traditional foil-type strain gauge serving as reference data, and the bottom row is from the actual measurement of the capacitive strain sensor board when used with the 1"× 1" SEC sensor. As can be seen in Fig 2, linear relationship between two data is clearly observed with a lot less noise.

The improvement can be attributed to two reasons: 1) reduced sensor size which allows higher gain and 2) grounded sensor configuration. Next steps include the incorporation of the grounded sensor configuration in the new prototype board and further testing of the grounded scheme with different sizes of the SEC sensors.

Circumstance affecting project or budget. (Please describe any challenges encountered or anticipated that might the completion of the project within the time, scope and fiscal constraints set forth in the agreement, along with recommended solutions to those problems).

None.